

Swept Volume-Based Continuous Object Gathering Trajectory Generation for Tethered Robot Duo

Yuanyuan Du¹, Jianan Zhang², Xiang Cheng², and Shuguang Cui³

Abstract—We propose a continuous gathering scheme based on the swept volume to address the challenges involved in planning a tethered robot duo to efficiently collect marine debris. Specifically, we model the tethered robot duo by constructing a double-layer U-shape, and then apply an object-aware optimization approach that leverages the swept volume signed distance field (SVSDF) to guide trajectory optimization, promoting complete object collection while maintaining a continuous and collision-free gathering motion. Existing algorithms either fail to fully address key challenges, such as assuming an unrealistically infinite tether length or incurring high computational costs. In contrast, our proposed method, by adopting the double-layer U-shape technique, effectively manages tether length constraints and preserves the tether shape, ensuring feasible collection. By utilizing the SVSDF technique to guide the trajectory optimization process, we maximize the swept coverage of objects while minimizing that of obstacles. This enables complete object coverage, avoids collisions, and prevents the tether from becoming trapped by obstacles during the collection process. Moreover, we propose a set of metrics for this gathering planning problem and validate the generated trajectories in simulation, using a collision-free multi-UAV information-gathering approach to efficiently estimate the target area. Simulations demonstrate that our proposed method achieves superior, resolution-independent gathering performance compared to existing algorithms.

I. INTRODUCTION

Autonomous ocean cleaning is an emerging challenge in robotics, involving the efficient collection of floating debris over large ocean areas. Inspired by the *Ocean Cleanup Project*, we propose a novel approach using a duo of tethered autonomous robots to address this problem. Tethered robots

This work was supported in part by the National Natural Science Foundation of China under Grants 62341101, 62301011 and 62125101; in part by the Basic Research Project No. HZQB-KCXYZ-2021067 of Hetao Shenzhen-HK S&T Cooperation Zone, the Shenzhen Outstanding Talents Training Fund 202002, the Guangdong Research Projects No. 2017ZT07X152 and No. 2019CX01X104, the Guangdong Provincial Key Laboratory of Future Networks of Intelligence (Grant No. 2022B1212010001), and the Shenzhen Key Laboratory of Big Data and Artificial Intelligence (Grant No. ZDSYS201707251409055); the New Cornerstone Science Foundation through the Xplorer Prize, and the Fundamental Research Funds for the Central Universities, Peking University. (*Corresponding author: Jianan Zhang*)

¹The Shenzhen Future Network of Intelligence Institute (FNii-Shenzhen), the School of Science and Engineering (SSE), and the Guangdong Provincial Key Laboratory of Future Networks of Intelligence, the Chinese University of Hong Kong (Shenzhen), Guangdong 518172, China. 220019057@link.cuhk.edu.cn.

²The State Key Laboratory of Photonics and Communications, School of Electronics, Peking University, Beijing, China. {zhangjianan, xiangcheng}@pku.edu.cn.

³SSE, FNii-Shenzhen, and the Guangdong Provincial Key Laboratory of Future Networks of Intelligence, the Chinese University of Hong Kong (Shenzhen), Guangdong 518172, China. shuguangcui@cuhk.edu.cn.



Fig. 1. Inspired by the *Ocean Cleanup Project*, we propose a novel method, based on the swept volume concept, to address this problem using a duo of tethered autonomous robots. The area shaded in light yellow highlights the swept volume of the tethered robot duo during gathering.

have been widely applied in tasks such as manipulation [1], transportation [2], [3], and inspection [4]. In the ocean cleaning task, using a tether as a net, two robots can work together to cover a larger area and collect scattered debris more effectively than a single robot, as shown in Fig. 1.

Despite its efficiency, using a tethered robot duo presents unique challenges that must be addressed. In the case of a single robot [5], the task typically involves efficiently gathering all objects while avoiding collisions with obstacles. However, for a tethered robot duo [4], [6], physically connected by a non-rigid tether, cooperative trajectory planning is essential to ensure effective gathering, preventing the tether from tangling or getting damaged. These factors impose additional planning constraints, such as enforcing tether length limits and ensuring obstacle avoidance for both the robots and the tether to prevent entanglement [7]. Moreover, maintaining the proper shape of the tethered system [2], [8], [9] is critical for effective debris collection, particularly in the often scattered and expansive marine environments.

Due to these unique challenges, common single-robot planners struggle to generate satisfactory trajectories for tethered robot duos. Existing approaches [4], [6], [5], [7] focused on collision-free object collection for tethered robot systems address some of these challenges. However, these methods are either limited in scope—e.g., assuming infinite tether length, simplifying object shapes, relying on discrete states, and facing resolution issues—or are computationally intensive [7]. Our approach aims to overcome these limita-

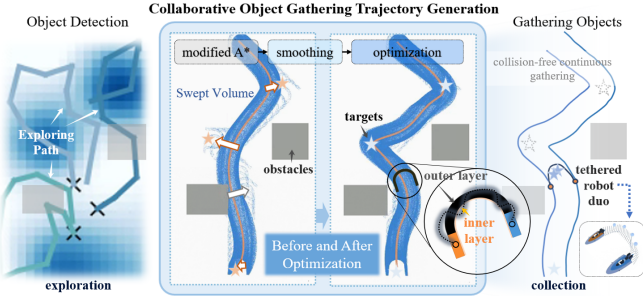


Fig. 2. An illustration of the SVCG scheme in a simple gathering scenario involving three target objects. This approach enables the generation of collaborative, collision-free gathering trajectories, allowing the tethered robot duo to efficiently collect scattered objects. Furthermore, a collision-free multi-UAV information-gathering method is employed to estimate the locations of the target objects.

tions by developing an efficient algorithm that optimizes the robots' trajectories, ensuring effective debris collection while addressing the complexities of tethered cooperation.

We propose a swept volume-based continuous gathering algorithm (SVCG), as shown in Fig. 2, designed to efficiently collect scattered objects using a tethered robot duo in large, obstacle-rich environments. Inspired by advancements in whole-body planning [10], we introduce an object-aware optimization approach that utilizes the swept volume signed distance field (SVSDF) to guide trajectory optimization. In summary, the tethered robot duo is simplified for efficiency as a double-layer U-shape (Fig. 4). This planning formulation maintains an ideal net shape while satisfying the maximum tether length constraint. The swept volume (SV) [11] compactly describes the space occupied by the shape's movement, implying that, ideally, objects to be gathered should lie within the SV of the inner layer, while obstacles to be avoided should remain outside the SV of the outer layer during the gathering process. By maximizing the swept coverage of objects and minimizing that of obstacles, SVCG facilitates complete object coverage while ensuring continuous, collision-free gathering motion. Additionally, a collision-free multi-UAV information-gathering method is further implemented to estimate the target locations. The main contributions of this paper are as follows.

- 1) **SV-Based Continuous Gathering:** Leveraging the SVSDF concept to guide efficient collaborative gathering planning in large, obstacle environments.
- 2) **Double-layer U-shape technique:** Adopting a double-layer U-shape for trajectory planning to effectively manage tether length constraints and maintain tether shape, ensuring feasible and efficient collection.
- 3) **Gathering Performance:** Introducing a holistic performance measure tailored for object gathering with a tethered robot duo, evaluating system efficiency and effectiveness. The SVCG method demonstrates state-of-the-art gathering performance.

II. RELATED WORK

Tethered robots are widely used in various tasks [1], [2], [3], [5], but the planning problem of gathering with a pair of tethered robots has been less explored. Early



Fig. 3. Maintaining the tether shape precisely and directly is often unnecessary and requires significant effort. Previous methods, therefore, focus on maintaining the distance between robots, as being too close or too far apart hinders effective object collection. The SVCG method goes a step further by maintaining the two endpoints of a U-shape during trajectory planning, ensuring that the tethered system remains in a functional shape, which is crucial for efficient debris collection.

approaches treated it as an object-and-obstacle separation problem, assuming unrealistic infinite separation distances [6], or focused on specific tether lengths [4], but neglected obstacle avoidance and tether shape maintenance. Maintaining the tether shape is crucial for effective collection, but precise control is complex and often unnecessary. Therefore, a U-shape cost function was proposed in [7] to help maintain a proper distance between robots and enable indirect shape control during gathering. However, maintaining distance alone does not guarantee proper shape preservation, which may lead to loss of objects, as illustrated in Fig. 3.

The method proposed in [7] presents two additional concerns: 1) It uses merged circles to approximate objects for gathering, which may be much larger than their actual size. This introduces extra overhead and can lead to overly conservative trajectories. 2) It adopts discretized continuous motion, which has resolution issues. Low-resolution discretization can cause gaps in gathering and collision checks, whereas high-resolution significantly increases complexity. Additionally, it assumes that the exact positions of objects are known, but exploration is often required, especially in the context of marine debris collection. An intent-based method from [12] allows agents to collaboratively build a global belief map through adaptive exploration, but it overlooks agent collisions. Our algorithm leverages recent advances in SVSDF [10] and informative exploration, enabling collision-free continuous gathering without the need for complex environmental representations or object simplifications.

III. PROBLEM FORMULATION

We address the problem of planning an efficient trajectory for collecting scattered marine debris in a vast, obstacle-filled sea area $M \subseteq \mathbb{R}^2$. The environment is defined by an indicator function $M(p)$, where:

$$M(p) = \begin{cases} 1, & \text{if } p \text{ is an obstacle,} \\ 0, & \text{if } p \text{ is open space.} \end{cases}$$

The precise locations of the debris are initially unknown and are represented as a set:

$$\mathcal{P} = \{p_i \in \mathbb{R}^2 \mid i = 1, 2, \dots, K\} \in \mathbb{R}^{K \times 2}.$$

These locations are explored and identified by a fleet of N_{UAV} unmanned aerial vehicles (UAVs). Once the debris

locations are determined, a pair of tethered boat robots, connected by a net of fixed length d_{\max} , are deployed to collect the debris. The robot, simplified as a rectangle [13], [14], must navigate from an initial configuration $(x_s, y_s, \theta_s) \in \mathbb{SE}(2)$ to collaboratively collect all identified debris with its partner, while avoiding obstacles. Furthermore, a key constraint is that the net must not enclose any obstacles at any point during the retrieval task. Thus, the problem involves optimizing both the coordinated motion of the tethered robots and the exploration strategy of the UAVs, to ensure efficient debris collection while adhering to the net length constraint. In this paper, the minimum control effort polynomial trajectory class (MINCO) [15] $\mathcal{T}_{\text{MINCO}}$ is adopted to represent the trajectories in trajectory generation and optimization for the tethered robot duo.

$$\mathcal{T}_{\text{MINCO}} = \{p(t) : [0, \sum_{i=1}^M T_i] \rightarrow \mathbb{R}^m | \mathbf{c} = \mathcal{M}(\mathbf{q}, \mathbf{T}), \quad (1)$$

$$\mathbf{q} = (\mathbf{q}_1, \dots, \mathbf{q}_{M-1}) \in \mathbb{R}^{(M-1) \times m}, \quad (2)$$

$$\mathbf{T} = (T_1, \dots, T_M)^T \in \mathbb{R}_{>0}^M, \quad (3)$$

$$\mathbf{c} = (\mathbf{c}_1^T, \dots, \mathbf{c}_M^T)^T \in \mathbb{R}^{M \times (N+1) \times m}\}, \quad (4)$$

where $p(t)$ is an m -dimensional M -segment N -degree polynomial trajectory, \mathbf{q} are the intermediate waypoints, \mathbf{T} are the allocated times, with the total time computed as $\sum_{i=1}^M T_i$, and \mathbf{c} are the polynomial coefficients which are determined by the intermediate waypoints \mathbf{q} and the allocated time for each polynomial segment \mathbf{T} . The mapping $\mathcal{M}(\mathbf{q}, \mathbf{T})$ constructed as in [15], [10] converts the trajectory representation from (\mathbf{q}, \mathbf{T}) to (\mathbf{c}, \mathbf{T}) .

$$p(t) = p_i(t - t_{i-1}) \quad \forall t \in [t_{i-1}, t_i), \\ p_i(t) = \mathbf{c}_i^T \beta(t) \quad \forall t \in [0, T_i),$$

where $p_i(t)$ is the i^{th} segment of the trajectory, $\mathbf{c}_i \in \mathbb{R}^{(N+1) \times m}$ is the coefficient matrix of the polynomial, and $\beta(t) = [1, t, \dots, t^N]^T$ is the natural basis.

IV. PRELIMINARY REQUIREMENTS

The SV [11] is generated by the continuous motion of the potentially time-varying shape $M(t)$ along the trajectory $\mathcal{T}(t)$, and is defined as

$$\mathcal{SV}_{B(t)} = \cup_{t \in [t_s, t_e]} \mathcal{B}(t),$$

where $\mathcal{B}(t) = \mathcal{T}(t)M(t)$ represents the configuration of $M(t)$ at time t . $\mathcal{SV}_{B(t)}$, compactly describes the space occupied by $M(t)$'s continuous motion, capturing both the minimal safe space required and the maximal space covered during its movement. This implies that continuous gathering ideally requires $\mathcal{SV}_{B(t)}$ to enclose all objects of interest.

The time-varying function, $\mathcal{SDF}_{B(t)} : \mathbb{R}^2 \rightarrow \mathbb{R}$ is used as the metric to evaluate $\mathcal{SV}_{B(t)}$:

$$\begin{cases} \mathcal{SDF}_{B(t)}(x) < 0 : x \in \mathcal{B}(t), \\ \mathcal{SDF}_{B(t)}(x) > 0 : x \notin \mathcal{B}(t). \end{cases}$$

The signed distance of a query point x with respect to $\mathcal{SV}_{B(t)}$, denoted by $f^*(x) = \min_t \mathcal{SDF}_{B(t)}(x)$, represents

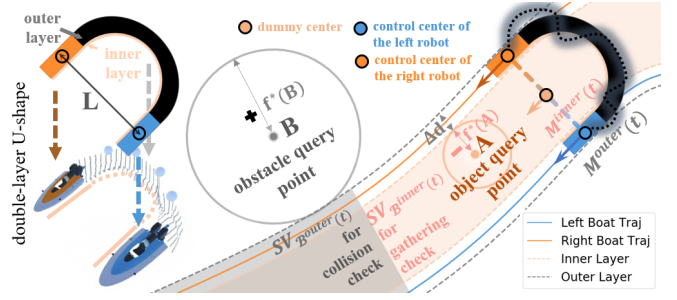


Fig. 4. In the top-down view, the boat robot is approximated as a rectangle, while the tethered robot duo is approximated as a double-layer U-shape. The smaller the value of f^* , the closer the point is to the SV. A negative signed distance indicates that the queried point (e.g., point A) lies inside $\mathcal{SV}_{B(t)}$ at some time t , while a positive signed distance indicates that the point (e.g., point B) lies outside. A positive signed distance for any object point or a negative signed distance for any obstacle point is not expected.

its minimal distance to the shape $M(t)$. This motivates using the SVSDF of the tethered robot duo's shape to efficiently compute gathering-related penalties during numerical optimization, guiding the SV toward object points for collaborative trajectory generation. The signed distance function $\mathcal{SDF}_{B(t)}(x)$ and its gradient $\nabla \mathcal{SDF}_{B(t)}|_x$ at any query point x of interest can be computed in microseconds using the method proposed in [10], which effectively guides trajectory optimization.

V. SV-BASED CONTINUOUS GATHERING (SVCG)

Applying SVSDF to tethered robots gathering problem presents challenges due to the tether's deformable and coupled nature, making precise swept volume modeling both difficult and computationally expensive. To address this, we represent the robot duo with a double-layer U-shape abstraction. Furthermore, we augment the objective function with task-specific costs—such as gathering efficiency and orientation consistency—to better support object-aware, tether-constrained planning in cluttered marine environments.

A. Double-layer U-shape

Gathering objects with the robot duo requires maintaining the shape of the flexible tether connecting the robots, though not exactly. Directly using the exact top-view area of the tethered robot duo as $M(t)$ can be complex and unnecessary. Therefore, as shown in Fig. 4, a simplified double-layer U-shape model, constructed by stacking two U-shapes, $M^{\text{outer}}(t)$ and $M^{\text{inner}}(t)$, with a fixed distance Δd between them, is used instead. This approach enables efficient cooperative trajectory planning by allowing the robots to move side by side, thereby minimizing interference and collision risks as well as reducing tether entanglement. Ideally, the objects to be collected should lie within the SV of the inner layer $\mathcal{SV}_{B^{\text{inner}}(t)}$, while obstacles should remain outside the SV of the outer layer $\mathcal{SV}_{B^{\text{outer}}(t)}$, ensuring a collision-free gathering process. It is important to note that the double-layer U-shape assumes that the individual robot's shape (approximated by a rectangle) remains constant during motion, but it does not imply a rigid tether between the robots. Rather, its primary purpose is to efficiently plan the

cooperative trajectories of the robot duo, without modeling the tether's physical properties or controlling its exact shape. When the shape's orientations are aligned with the trajectory direction, the SVSDF calculations for the inner and outer layers typically satisfy the relationship

$$f_{\text{outer}}^* = f_{\text{inner}}^* + \Delta d.$$

This double U-shape model effectively supports trajectory planning for the robot duo.

B. SV-based Gathering Trajectory Optimization

The non-convex nature of the gathering problem necessitates a well-designed initialization to ensure convergence to a feasible solution. Specifically, the initial trajectory parameters c_{init} , T_{init} are obtained by fitting the waypoints \mathbf{q}_{A^*} and time allocations \mathbf{T}_{A^*} obtained from an initial trajectory

$$\mathcal{L}_{A^*} = \{(x_i, y_i, \theta_i) \in \mathbb{SE}(2) \mid i = 1, 2, \dots, N\}$$

to a MINCO trajectory $\mathfrak{T}_{\text{MINCO}}^{\text{init}}$. The initial trajectory \mathcal{L}_{A^*} is generated using a modified A* algorithm, where neighbors of the current node are redefined as spatially adjacent nodes with the closest collision-free and acceptable attitudes. Formally, given a current node with attitude θ_c , the attitude θ_n of its valid neighbor is selected such that:

$$\theta_n = \arg \min_{\theta \in \Theta_{\text{valid}}} |\theta - \theta_c|, \quad \text{s.t.} \quad |\theta_n - \theta_c| \leq \delta_\theta,$$

where Θ_{valid} is the set of all collision-free attitudes in the neighborhood, and δ_θ is a predefined threshold ensuring smooth attitude transitions. If no valid θ_n satisfying $|\theta_n - \theta_c| \leq \delta_\theta$ exists, then the neighbor is considered unacceptable.

Note that gathering with a tethered duo is a comprehensive task involving the collection of all objects while maintaining the correct distance between the robots, preserving the net's shape, avoiding collisions, and preventing the duo from getting trapped by obstacles. Therefore, we not only evaluate but also improve the existing SVSDF [16], [17], [10] formulation to ensure that the swept volume fully avoids obstacles while enclosing the entire area of interest, thereby enhancing collision-free gathering trajectories. To summarize, the final trajectory generation is formulated as the following optimization problem:

$$\min_{\mathbf{c}, \mathbf{T}} \lambda_g J_g + \lambda_o J_o + \lambda_e J_e + \lambda_d J_d, \quad (5)$$

where J_g , J_o , J_e , and J_d denote the objectives for collection, collision avoidance, energy saving, and dynamic feasibility, respectively, with their corresponding weights λ_g , λ_o , λ_e , and λ_d . Note that the gradients of J_e and J_d with respect to \mathbf{c} and \mathbf{T} , including $\frac{\partial J_e}{\partial \mathbf{c}, \mathbf{T}}$ and $\frac{\partial J_d}{\partial \mathbf{c}, \mathbf{T}}$, have been rigorously derived in [10] and will not be revisited in this paper.

Collection and Collision Avoidance: The cost functions for collection and collision avoidance employ nearly opposite design principles. The derived J_o and J_g functions are designed to deform the trajectory away from obstacles and toward the objects to be gathered.

$$J_g = \sum_i \mathcal{L}_\mu [f_{\text{inner}}^*(\mathbf{x}_g^i) - \epsilon_g], \quad (6)$$

where \mathbf{x}_g^i is the object point, with a gathering threshold $\epsilon_g < 0$, \mathcal{L}_μ is the smoothing function. The gradients are:

$$\frac{\partial J_g}{\partial \mathbf{c}, \mathbf{T}} = \begin{cases} \sum_i \dot{\mathcal{L}}_\mu \frac{\partial f_{\text{inner}}^*(\mathbf{x}_g^i)}{\partial \mathbf{c}, \mathbf{T}}, & f^*(\mathbf{x}_g^i) \geq \epsilon_g \\ 0, & f^*(\mathbf{x}_g^i) < \epsilon_g \end{cases} \quad (7)$$

Moreover, the two robots should move in parallel to gather objects effectively. Therefore, the cost J_h is further added to J_g : $J_g : J_g = J_g + \lambda_h J_h$

$$J_h = \int \mathcal{L}_\mu [(\Delta \theta_t)^2] dt,$$

$$\Delta \theta_t = \arctan\left(\frac{v_y(t)}{v_x(t)}\right) - \theta(t),$$

where $\theta(t)$ is the orientation of the U-shape at time t , and $v_x(t)$, $v_y(t)$ represent the velocities of the U-shape in the x- and y-directions at time t . The gradients are:

$$\frac{\partial J_h}{\partial \mathbf{c}, \mathbf{T}} = \int 2\dot{\mathcal{L}}_\mu \Delta \theta_t \left[\frac{\partial \arctan(\frac{v_y}{v_x})}{\partial \mathbf{c}, \mathbf{T}} \cdot \frac{\partial (\frac{v_y}{v_x})}{\partial \mathbf{c}, \mathbf{T}} - \frac{\partial \theta(t)}{\partial \mathbf{c}, \mathbf{T}} \right] dt. \quad (8)$$

$$\frac{\partial \arctan(\frac{v_y}{v_x})}{\partial \mathbf{c}, \mathbf{T}} = \frac{1}{1 + (v_y/v_x)^2}, \quad (9)$$

$$\frac{\partial}{\partial \mathbf{c}, \mathbf{T}} \left(\frac{v_y}{v_x} \right) = \frac{v_x \frac{\partial v_y}{\partial \mathbf{c}, \mathbf{T}} - v_y \frac{\partial v_x}{\partial \mathbf{c}, \mathbf{T}}}{v_x^2}. \quad (10)$$

The collision avoidance penalty is given by:

$$J_o = \sum_j \mathcal{L}_\mu [\epsilon_o - f_{\text{outer}}^*(\mathbf{x}_o^j)],$$

where \mathbf{x}_o^j is the obstacle point, with a safety threshold $\epsilon_o > 0$, and \mathcal{L}_μ is the smoothing function. SVSDF provides a quick generation of gradients at object and obstacle points, guiding trajectory optimization. The gradients of J_o are:

$$\frac{\partial J_o}{\partial \mathbf{c}, \mathbf{T}} = \begin{cases} \sum_i \dot{\mathcal{L}}_\mu \frac{\partial f_{\text{outer}}^*(\mathbf{x}_o^i)}{\partial \mathbf{c}, \mathbf{T}}, & f^*(\mathbf{x}_o^i) \leq \epsilon_o \\ 0, & f^*(\mathbf{x}_o^i) > \epsilon_o \end{cases} \quad (11)$$

Energy Saving: Minimizing the integral of the trajectory's third-order derivative to ensure smoothness and also minimizes total execution time, with weights λ_m and λ_t .

$$J_e = \lambda_m \int \| \ddot{p}(t) \|^2 dt + \lambda_t \sum_i T_i. \quad (12)$$

Dynamical Feasibility: To ensure dynamical feasibility, we impose constraints on the maximum velocity v , acceleration a , angular velocity ω , and angular acceleration α . These constraints prevent the trajectory from exceeding the physical limitations of the robot. The cost function for dynamical feasibility is defined as:

$$J_d = \int \left[\mathcal{C}(v(t)^2 - v_{\max}^2) + \mathcal{C}(a(t)^2 - a_{\max}^2) \right. \\ \left. + \mathcal{C}(\omega(t)^2 - \omega_{\max}^2) + \mathcal{C}(\alpha(t)^2 - \alpha_{\max}^2) \right] dt, \quad (13)$$

where $\mathcal{C} = \max(0, \cdot)$, and the maximum allowable values for velocity, acceleration, angular velocity, and angular acceleration v_{\max} , a_{\max} , ω_{\max} , α_{\max} are determined based on the

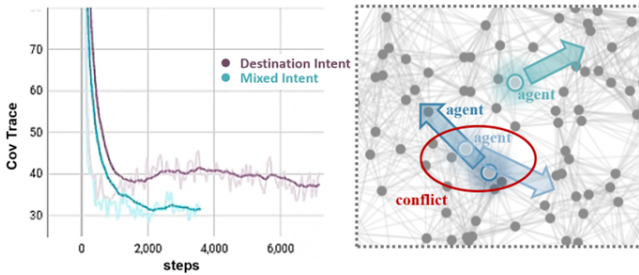


Fig. 5. Destination Intent vs. Mixed Intent. The right figure shows that the probability intent, which aggregates the agent's set of sampled predicted trajectories, helps to inform medium- to long-term future positions. However, this approach risks collisions when two robots are close to each other due to the lack of accurate occupancy information.

TABLE I

COMPARISON IN TERMS OF THE COLLISION RATE AND THE REMAINING COVARIANCE IN HIGH-INTEREST AREAS FOR 3 AGENTS.

Budget: 2	Destination Intent	Mixed Intent (ours)
Covariance	31.81	29.44
Collision Rate (%)	0.34	0.25

robot duo's physical constraints. Specifically, considering the double-layer U-shape configuration, these limits are set as follows:

$$\omega_{\max} = \omega_{\max}^{\text{robot}}, \quad v_{\max} = v_{\max}^{\text{robot}} - \frac{L}{2}\omega_{\max},$$

where L represents the preferred inter-robot distance. The two robots are required to maintain a formation with distance L , where their positions p_l, p_r are symmetrically defined on either side of the optimized central reference trajectory. Each reference point on the central trajectory is represented as $p_c = [x, y, \theta]^\top$ (dummy center). The two robots' reference positions are then given by:

$$p_{l,r} = \begin{bmatrix} x \\ y \\ \theta \end{bmatrix} + \frac{L}{2} \begin{bmatrix} \cos(\theta \pm \frac{\pi}{2}) \\ \sin(\theta \pm \frac{\pi}{2}) \\ 0 \end{bmatrix}.$$

C. Collision-Free Informative Exploration

Marine debris is often scattered over a wide area, so an efficient information-gathering technique is required to determine the positions of the objects to be collected. We developed a collision-free, intent-based multi-UAV path planning method for active searching based on recent works [12]. The combined graph observed by agent i , denoted as G'^i , contains all available information about the entire area and other observed agents. The vertex $v_j'^i \in V'^i$ of the combined graph is redefined to provide an exact collision avoidance-related representation:

$$v_j'^i = \{p(v_j^i), b(v_j^i), m(v_j^i)\},$$

where p maps to node locations, b maps to the agent's current belief, and m maps to a mixed probability intent provided by other agents. Specifically, the mixed probability intent $m(v_j^i)$ is formed by stacking the other agents' recently occupancy data $o(v_j^i)$ onto the probability intent. We introduce a continuous-time collision check technique based on [18],

assigning a penalty r_o for any detected collisions. Building upon [12], we propose this mixed intent distribution. Our approach enhances cooperative exploration while reducing potential conflicts, leading to improved overall exploration performance, as verified in Fig. 5 and Table I.

VI. SIMULATIONS

This work is designed for marine debris collection using a tethered robot duo for future ocean cleanup. However, due to hardware limitations, we rely on simulations (UNITY simulator, as shown in Fig. 8) to validate the performance. First, we propose a set of evaluation metrics, as no well-established performance metrics currently exist for this specific task, and then evaluate our algorithms across various gathering scenarios. The results in Table III demonstrate that SVCG outperforms baseline methods by achieving higher success and collection rates, improving efficiency, and reducing collisions and entanglements. Moreover, it requires less computational effort for both planning and execution.

A. Performance Metrics and Baselines

As detailed in Table II, safety is evaluated using the Success Rate (SR), Collision Rate (CR), and Trapped Rate (TR). Execution efficiency is assessed via Execution Time, Average Speed, and Average Acceleration, while Computational Time (TIME) measures algorithmic efficiency. For collection effectiveness, we introduce the Collection Rate (OR), Shape Maintenance Rate (MR), and Dangerous Rate (DR), which assess both object gathering and tether management. We compare our method with Tethered-DUO (**T-DUO**) [7], the separation-based baseline (**Separation**) [6], [19], which ignores separation distance constraints, and the fixed distance baseline (**Distance¹**) [4] which imposes a hard constraint on the separation distance. Additionally, we compare with **SVSDF** [10], using the same A* initialization as in SVCG. All algorithms are implemented with our proposed exploration strategy for object detection.

B. Gathering Scenarios

The gathering task difficulty mainly depends on object distribution, obstacle density, and map size. We first conduct experiments on a small, open map (Scenario 1), then progressively scale up to a larger map with several square obstacles (Scenario 2), and subsequently move to a more complex scenario that mimics a real-world environment (Scenario 3). For each map configuration, we test five random layouts of objects, and each configuration is tested three times. The robot's maximum velocity is set to 3 m/s, since higher speeds may cause some objects to be missed. The preferred distance $d_{\text{pref}} = 2 \cdot d_{\max}/\pi$ is set to 3 m. The thumbnails for these scenarios are provided in the leftmost column of Table III.

¹Since it was not designed specifically for object gathering and might enclose obstacles, we implemented it using T-DUO with a hard desired distance constraint for comparable performance.

TABLE II

PERFORMANCE METRICS FOR OBJECT GATHERING AND TETHER MANAGEMENT IN TETHERED ROBOT DUO: A COMPREHENSIVE EVALUATION OF SAFETY, EFFICIENCY, AND COLLECTION EFFECTIVENESS.

Purpose	Metric	Expression	Description
Safety	SR	N_s/N	The ratio of gathering tasks that result in available trajectory plans, if such plans exist.
	CR	N_c/N	The ratio of the number of tasks that result in collisions with the partner robot or obstacles N_c (as shown in Fig. 6) to the total number of tasks N evaluated.
	TR	N_t/N	The ratio of the number of tasks that result in being trapped by obstacle N_t (as shown in Fig. 6) to the total number of tasks N evaluated.
Efficiency	Exe Time (s)	T	The total execution time of the gathering task.
	Avg Spd (m/s)	$1/T \cdot \int_0^T v(t) dt$	The average (linear and angular) speed during the gathering process.
	Avg Acc (m/s ²)	$1/T \cdot \int_0^T a(t) dt$	The average (linear and angular) acceleration during the gathering process.
(Algorithmic)	TIME (s)	t	The computational time t for generating a solution.
Collection	OR	k/K	The ratio of collected objects k to total scattered objects K .
	MR- $d_{\text{pref},\delta}$ (%)	$T_M/T \times 100$	The ratio of the time during which the ideal net shape is maintained (as shown in Fig. 6) throughout the gathering process, where T_M is the time when the distance d between the two robots satisfies $0.9 \cdot d_{\text{pref}} \leq d \leq 1.1 \cdot d_{\text{pref}}$, and the maximum angle difference between the two robots and the DUO direction is less than δ , relative to the total time T . Better shape maintenance leads to more effective object gathering and reduces the risk of collisions between robots and tether entanglement.
	DR- d_{max} (%)	$T_D/T \times 100$	The ratio of being too far from the partner (as shown in Fig. 6), where $d \geq d_{\text{max}}$, during the gathering process.

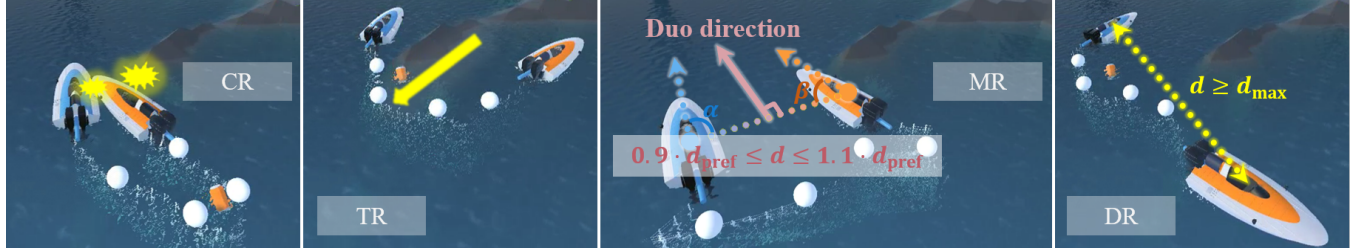


Fig. 6. Illustrative cases for performance metrics in object gathering: (From left to right) 1) Collision with the partner robot or obstacles in the environment, related to **CR**; 2) Trapping by obstacles, where the robots become trapped by surrounding obstacles during the gathering process, related to **TR**; 3) Shape maintenance, including the proper distance between the robot duo and the heading alignment of each robot, related to **MR**; 4) Exceeding maximum distance, where it becomes dangerous if the distance between the robots exceeds the predefined maximum limit during the gathering process, related to **DR**.

C. Results Analysis

1) *Continuous vs. discrete gathering planning:* Discrete planning methods approximate continuous motion through discrete sampling moments, which theoretically risks missing collection detections and struggles with resolution sensitivity (see Fig. 9 and Table III, **T-DUO** 2x vs. 1x). In contrast, **SVCG**, as a continuous planning strategy, achieves resolution-independent gathering planning.

2) *Computational time:* **T-DUO** evaluates collisions and collection in discrete states, which makes it computationally expensive. In contrast, **SVCG** avoids the need for risky discrete sampling by utilizing SVSDF, thus improving time efficiency. As shown in Table III, **SVCG** achieves the shortest time to generate a solution and is the only method capable of producing feasible gathering solutions for larger obstacle scenarios (Scenario 2 and 3) within an acceptable time.

3) *Object-aware technique is effective for complete gathering of all objects:* **SVCG** achieves a 100% collection rate in all evaluated scenarios by using an object-aware technique, where objects pull the trajectory toward themselves. In

contrast, **SVSDF** only ensures collision-free planning, while **T-DUO** may fail to meet its object constraint², resulting in missed objects, as shown in Fig. 7.

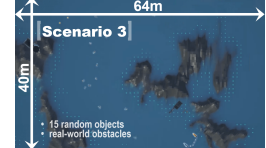
4) *Double-layer U-shape is effective for shape maintenance:* **SVCG** ensures effective shape maintenance during gathering, achieving a 100% shape maintenance rate. In contrast, **Distance** and **T-DUO** only consider the distance between robots, neglecting heading alignment, while **Separation** completely ignores the tether length limitations, as shown in Fig. 9, which is unrealistic. Based on most of the data, a higher MR is correlated with a higher OR, indicating that maintaining the shape is beneficial for effective gathering. This suggests that the MR metric is reasonable and reflects the importance of shape maintenance.

5) *Other shapes of objects:* Marine debris often includes many strip-like objects. Unlike methods such as **T-DUO**, which rely on minimum bounding circles to cover them (thus compromising feasible space), our algorithm avoids

²T-DUO requires that the centers of all object circles be covered by the quadrilaterals formed by connecting the points on both sides of the path.

TABLE III

PERFORMANCE COMPARISON ACROSS THREE INCREASINGLY CHALLENGING SCENARIOS (AS SHOWN IN THE LEFTMOST COLUMN) FOR OBJECT GATHERING, INCLUDING A REAL-WORLD-LIKE LAYOUT WITH 15 OBJECTS (SCENARIO 3, FIG. 7). OVERALL, SVCG DEMONSTRATES SUPERIOR PERFORMANCE ACROSS ALL SCENARIOS. PLANNING TIME LIMIT: 1800 S.

Scenario	Algorithm	Safety			Efficiency			Collection			
		SR	CR	TR	Exe Time	Avg Spd	Avg Acc	TIME	OR	MR	DR
	Distance	5/5	0	0	43.66	0.50 / 0.07	0.30 / 0.11	14.84	4/5	88.14	0
	T-DUO 2x	5/5	0	0	65.86	0.38 / 0.08	0.20 / 0.07	18.13	4/5	49.20	0
	T-DUO 1x	5/5	0	0	46.04	0.49 / 0.10	0.26 / 0.08	8.84	4/5	46.39	0
	SVSDF	5/5	0	0	11.57	2.10 / 0.26	0.64 / 0.24	10.14	2/5	100	0
	SVCG	5/5	0	0	20.36	1.71 / 0.29	0.69 / 0.22	1.30	5/5	100	0
	Distance	4/5	1/5	0	172.15	0.32 / 0.05	0.06 / 0.06	178.81	10/10	78.26	0
	T-DUO 2x	2/5	1/5	0	104.50	0.61 / 0.10	0.33 / 0.05	579.62	9/10	54.21	1.50
	T-DUO 1x	3/5	1/5	0	88.70	0.67 / 0.08	0.32 / 0.08	284.43	7/10	62.48	0
	SVSDF	5/5	0	0	28.03	2.11 / 0.22	0.56 / 0.17	57.03	5/10	100	0
	SVCG	5/5	0	0	46.59	1.75 / 0.29	0.72 / 0.27	4.08	10/10	100	0
	Distance	2/5	0	0	149.10	0.54 / 0.06	0.12 / 0.05	306.78	10/15	57.12	0
	T-DUO 2x	0	0	0	—	—	—	—	—	—	—
	T-DUO 1x	1/5	0	0	103.2	0.64 / 0.04	0.14 / 0.04	400.81	12/15	70.87	0
	SVSDF	5/5	0	0	37.412	2.11 / 0.23	0.52 / 0.18	79.09	8/15	100	0
	SVCG	5/5	0	0	63.48	1.73 / 0.31	0.79 / 0.31	6.434	15/15	100	0

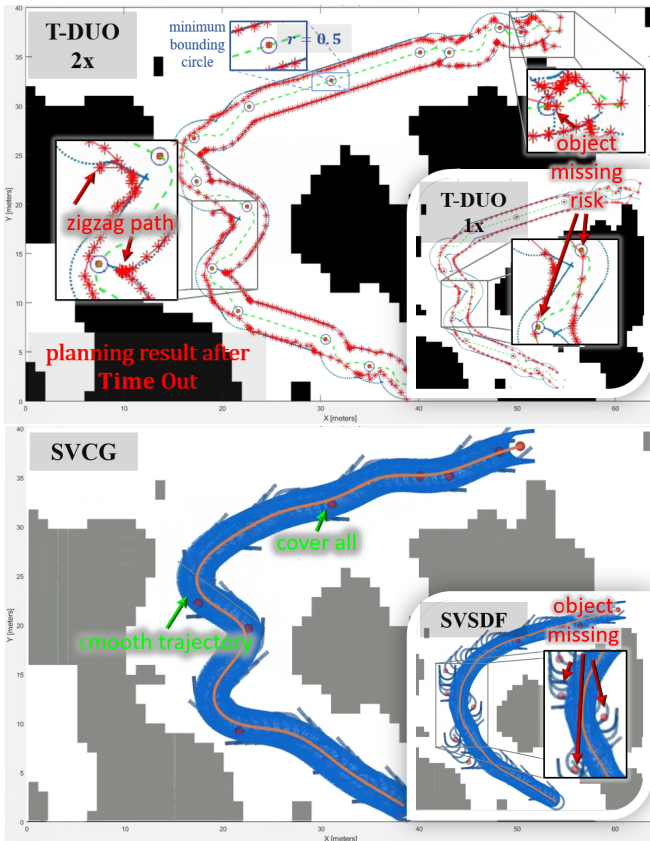


Fig. 7. Our algorithm generates a continuous, cover-all gathering trajectory, whereas T-DUO [7] produces a discrete path, which suffers from zigzagging and risks missing objects. SVSDF [10] optimizes a collision-free trajectory but does not explicitly consider object gathering.

such approximations. As shown in Fig. 9, SVCG effectively handles strip-like debris by sampling query points on the object and optimizing the trajectory to cover them, without oversimplifying the shape of the debris.

VII. CONCLUSIONS

In this paper, we present the SVCG method to optimize the gathering performance of tethered robot duos. By leveraging the compactness of the swept volume, SVCG covers the entire trajectory space and outperforms current state-of-the-art methods. Simulations demonstrate the capability of our algorithm in handling complex, continuous gathering tasks. To the best of our knowledge, this is the first approach that simultaneously achieves these results in motion trajectory generation for tethered robot duos. Similar to the approach in [7], we assume a preferred distance d_{pref} for the gathering task. This configuration may require adjustment for different scenarios, which can be addressed by tuning L or Δd , or by employing a double-layer U-shape with a time-varying L to adapt to changing conditions. This flexibility is supported by the SVSDF's capability to accommodate deformable shapes $M(t)$. Currently, SVCG does not consider increasing payload dynamics or the coordination of multiple tethered robot groups, which will be investigated in future work. Additionally, the current method assumes relatively calm sea conditions. Future research will focus on incorporating adaptive exploration strategies to manage dynamic marine environments, including wind fields and ocean currents.

REFERENCES

- [1] L. Yan, T. Stouraitis, and S. Vijayakumar, “Decentralized ability-aware adaptive control for multi-robot collaborative manipulation,” *IEEE Robotics and Automation Letters*, vol. 6, no. 2, pp. 2311–2318, 2021.

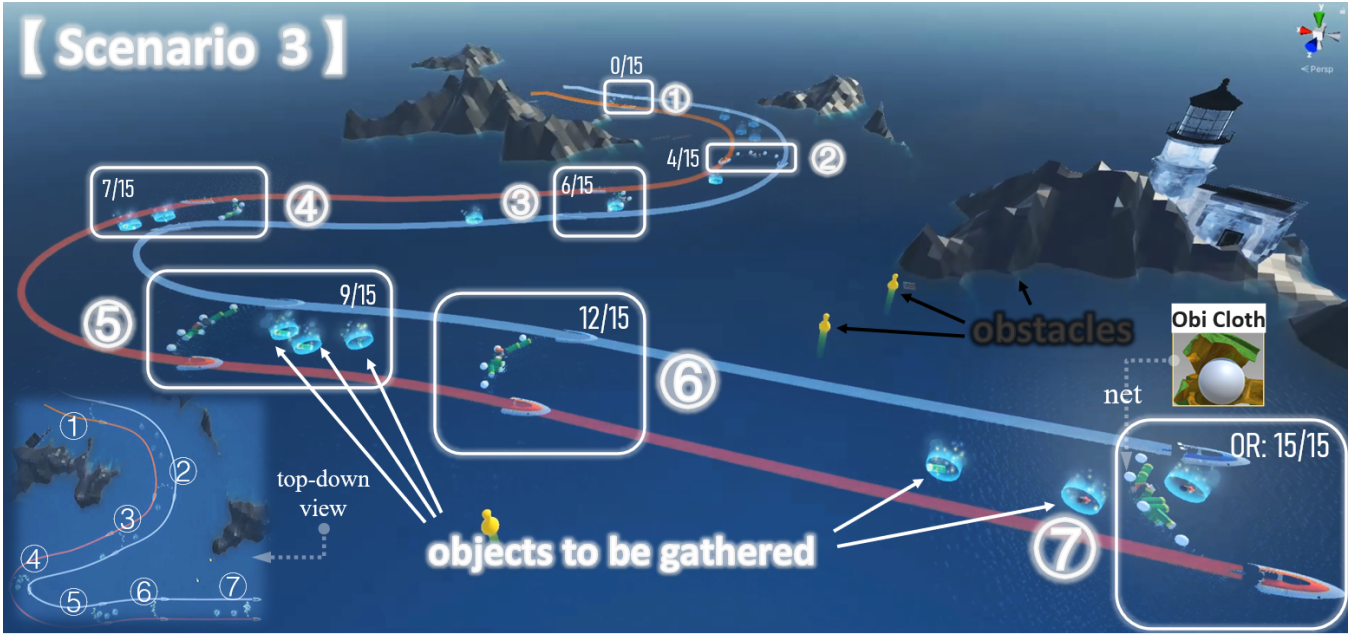


Fig. 8. The tethered robot duo is tasked with gathering 15 scattered objects in a real-world-like scenario. The boxes highlight key moments in chronological order. The bottom-left corner shows a top-down view, illustrating the overall trajectory. The net is simulated using the *Obi Cloth* plugin in Unity, providing a more realistic simulation of the net's deformation.

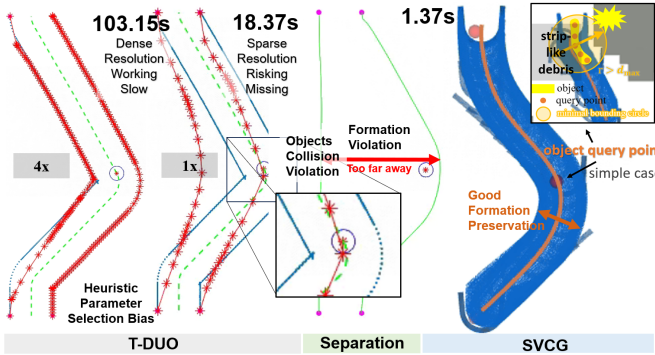


Fig. 9. SVCG demonstrates superior, resolution-independent gathering performance, while T-DUO is limited by resolution. Low-resolution discretization (1x) creates gaps in gathering checks, while high-resolution discretization (4x) introduces complexity. Additionally, the separation baseline suffers from formation violation issues.

- [2] D. S. D’antonio, G. A. Cardona, and D. Saldana, “The catenary robot: Design and control of a cable propelled by two quadrotors,” *IEEE Robotics and Automation Letters*, vol. 6, no. 2, pp. 3857–3863, 2021.
- [3] X. Zhang, F. Zhang, P. Huang, J. Gao, H. Yu, C. Pei, and Y. Zhang, “Self-triggered based coordinate control with low communication for tethered multi-uav collaborative transportation,” *IEEE Robotics and Automation Letters*, vol. 6, no. 2, pp. 1559–1566, 2021.
- [4] R. H. Teshnizi and D. A. Shell, “Motion planning for a pair of tethered robots,” *Autonomous Robots*, vol. 45, no. 5, pp. 693–707, 2021.
- [5] H. Zhi, B. Zhang, J. Qi, J. G. Romero, X. Shao, C. Yang, and D. Navarro-Alarcon, “Non-prehensile object transport by non-holonomic robots connected by linear deformable elements,” *IEEE Robotics and Automation Letters*, 2024.
- [6] S. Bhattacharya, S. Kim, H. Heidarsson, G. S. Sukhatme, and V. Kumar, “A topological approach to using cables to separate and manipulate sets of objects,” *The International Journal of Robotics Research*, vol. 34, no. 6, pp. 799–815, 2015.
- [7] Y. Su, Y. Jiang, Y. Zhu, and H. Liu, “Object gathering with a tethered robot duo,” *IEEE Robotics and Automation Letters*, vol. 7, no. 2, pp.

2132–2139, 2022.

- [8] P. Mitrano, D. McConachie, and D. Berenson, “Learning where to trust unreliable models in an unstructured world for deformable object manipulation,” *Science Robotics*, vol. 6, no. 54, p. eabd8170, 2021.
- [9] M. Laranjeira, C. Dune, and V. Hugel, “Catenary-based visual servoing for tether shape control between underwater vehicles,” *Ocean Engineering*, vol. 200, p. 107018, 2020.
- [10] J. Wang, T. Zhang, Q. Zhang, C. Zeng, J. Yu, C. Xu, L. Xu, and F. Gao, “Implicit swept volume sdf: Enabling continuous collision-free trajectory generation for arbitrary shapes,” *ACM Transactions on Graphics (TOG)*, vol. 43, no. 4, pp. 1–14, 2024.
- [11] D. Blackmore and M. C. Leu, “Analysis of swept volume via lie groups and differential equations,” *The International Journal of Robotics Research*, vol. 11, no. 6, pp. 516–537, 1992.
- [12] T. Yang, Y. Cao, and G. Sartoretti, “Intent-based deep reinforcement learning for multi-agent informative path planning,” in *2023 International Symposium on Multi-Robot and Multi-Agent Systems (MRS)*. IEEE, 2023, pp. 71–77.
- [13] T.-M. Liu and D. M. Lyons, “Leveraging area bounds information for autonomous decentralized multi-robot exploration,” *Robotics and Autonomous Systems*, vol. 74, pp. 66–78, 2015.
- [14] C. Zhang, N. Noguchi, and L. Yang, “Leader–follower system using two robot tractors to improve work efficiency,” *Computers and Electronics in Agriculture*, vol. 121, pp. 269–281, 2016.
- [15] Z. Wang, X. Zhou, C. Xu, and F. Gao, “Geometrically constrained trajectory optimization for multicopters,” *IEEE Transactions on Robotics*, vol. 38, no. 5, pp. 3259–3278, 2022.
- [16] S. Sellán, N. Aigerman, and A. Jacobson, “Swept volumes via space-time numerical continuation,” *ACM Transactions on Graphics (TOG)*, vol. 40, no. 4, pp. 1–11, 2021.
- [17] T. Zhang, J. Wang, C. Xu, A. Gao, and F. Gao, “Continuous implicit sdf based any-shape robot trajectory optimization,” in *2023 IEEE/RSJ International Conference on Intelligent Robots and Systems (IROS)*. IEEE, 2023, pp. 282–289.
- [18] A. Andreychuk, K. Yakovlev, P. Surynek, D. Atzmon, and R. Stern, “Multi-agent pathfinding with continuous time,” *Artificial Intelligence*, vol. 305, p. 103662, 2022.
- [19] S. Kim, S. Bhattacharya, H. K. Heidarsson, G. S. Sukhatme, and V. Kumar, “A topological approach to using cables to separate and manipulate sets of objects,” in *Robotics: Science and Systems*. Citeseer, 2013.